BIOMASS GROWTH RATE OF TREES FROM CAMEROON BASED ON ^{14}C ANALYSIS AND GROWTH MODELS

J B Tandoh[1,2] • F Marzaioli[1,3] • G Battipaglia[4] • M Capano[3,5] • S Castaldi[4] • B Lasserre[6] • M Marchetti[6] • I Passariello[5] • F Terrasi[1,5] • R Valentini[7]

ABSTRACT. The question of whether the rise in CO_2 levels observed during the industrial era has influenced the rates of tree biomass growth represents one of the main unsolved questions in the field of climate change science. In this framework, the African tropical forest represents one of the most important carbon (C) sinks, but detailed knowledge of its response to elevated CO_2 is still lacking, especially regarding tree growth rate estimations. A major limitation to determining growth rates in the African tropical region is that many trees lack seasonality in cambial activity determining annual growth rings. In this study, several species of trees characterizing the African tropical forest have been investigated to estimate their biomass growth rate by means of a procedure based on ^{14}C and growth models. A total of 71 subsamples were analyzed for a *Entandrophragma cylindricum* (sapele) tree, and 38 and 25 wood subsamples for *Erythrophleum suaveolens* (tali) and *Triplochiton scleroxylon* (ayous) trees, respectively, using radiocarbon measurements at the Centre for Isotopic Research on Cultural and Environmental Heritage (CIRCE). All measured modern samples were in agreement with the Southern Hemisphere (SH) ^{14}C bomb-spike curve. Observed preliminary results indicate a decrease in the growth rate of the sapele tree (~350 yr old) in the industrial period compared to the pre-industrial era. Growth rates for trees of the other 2 species were higher than sapele, with ayous being the fastest-growing species.

INTRODUCTION

The increasing levels of atmospheric CO_2 and concerns over future changes in climate have led to attempts to understand the impact of human-induced climatic changes on the C cycle by analyzing the impact of past climate on the pre-industrial C cycle using long-term climatic data sets. The effects, which can be observed from local to global scales, leave imprints on climatic proxies such as tree rings (Fritts 1976; McCarroll and Loader 2004), corals (Druffel 1997; Dunbar and Cole 1999), ocean sediments (Lamoureux and Bradley 1996), pollens, and ice cores (O'Brien et al. 1995).

In this study, given their key role of primary productivity in ecosystem structure and function, trees were used to reconstruct the terrestrial ecosystem response to climate change over a period spanning from the pre-industrial to present by comparing growth rate estimates. Tree growth can be defined as an increase in the height, weight, and volume of a species as a result of the formation of new cells (Reimers 1991). The rate of this growth is determined by environmental factors associated with inter- and intra-annual cycles.

For more than a century, tree-ring counting and crossdating have been used in dendrochronology to establish ages of trees and, often, to infer their growth rate. This experimental approach may be limited in environments where regular annual formation of tree rings is suppressed by climatic conditions, such as extreme temperature or precipitation regimes with no clearly defined dry season (Worbes 1989). The presence of distinct seasonal changes is the main prerequisite for trees forming growth rings. For this reason, studies in the African tropical equatorial regions providing tree

[1]Seconda Università di Napoli, Dipartimento di Matematica e Fisica, Caserta, Italy.
[2]Corresponding author. Email: Joseph.TANDOH@unina2.it.
[3]INNOVA, Centre for Isotopic Research on Cultural and Environmental Heritage, Caserta, Italy.
[4]Seconda Università di Napoli, Dipartimento di Scienze e Tecnologie per l'Ambiente la Biologia e la Farmacologia, Caserta, Italy.
[5]Seconda Università di Napoli, Dipartimento di Lettere e Beni Culturali, Santa Maria Capua Vetere, Caserta, Italy.
[6]Università degli Studi del Molise, Dipartimento di Bioscienze e Territorio, Pesche, Isernia, Italy.
[7]Università della Tuscia Department for Innovation in Biological, Agro-food and Forest Systems, Viterbo, Italy.

Proceedings of the 21st International Radiocarbon Conference edited by A J T Jull & C Hatté
RADIOCARBON, Vol 55, Nr 2–3, 2013, p 885–893

growth rates by means of dendrochronological techniques are scanty (Whitmore 1990). A helpful alternative experimental approach is represented by the determination of radiocarbon content of tree wood, which, when annual growth of rings is not certain, can be used as an independent verification of ring counting (Worbes 1989) or to estimate the synthesis year of the wood.

Recent concentrations of ^{14}C in the atmosphere can be attributed to both natural and anthropogenic activities. On a daily basis, ^{14}C is exchanged between the terrestrial biosphere and the ocean with the atmosphere, making it an active tracer for characterizing fluxes involved in the C cycle. Over different timescales, the activity of ^{14}C in the atmosphere has been mainly controlled by 4 predominant sources: 1) natural ^{14}C produced by interactions of cosmic rays in the upper atmosphere; 2) ^{14}C introduced into the troposphere due to bomb testing; 3) ^{14}C released by nuclear power plants; and 4) fossil-fuel CO_2 emissions (Currie et al. 2006). Since the beginning of nuclear weapons testing in 1955 in the Northern Hemisphere (NH), the $^{14}CO_2$ content in the atmosphere has been greatly enriched all over the world from a background level of about −10‰ ($\Delta^{14}C$; Stuiver and Polach 1977) in 1955 to a peak in 1964 (Hua et al. 1999), almost doubling background observed ^{14}C concentrations. Since then, bomb ^{14}C spike concentrations have decreased almost exponentially due to terrestrial and oceanic uptake, fossil-fuel dilution, and atmospheric mixing. This behavior provides a high-resolution curve for calibrating modern ^{14}C dates with uncertainty of 1 or 2 yr depending on the measurement year (Hua and Barbetti 2004).

Four bomb ^{14}C data sets have been identified from worldwide measurements for the 1955–1969 periods, identifying 4 characteristic ^{14}C signals for 3 zones of the Northern Hemisphere (NH1, NH2, and NH3) and the Southern Hemisphere zone (SH). These zones are not only influenced by latitudinal sources and sinks but also strongly related to atmospheric circulation and seasonal positions of Hadley cell boundaries and the Intertropical Convergence Zone (ITCZ; Hua and Barbetti 2004).

One of the consequences of actual climate change on tree growth might be stimulation due to the enrichment of CO_2 levels in the atmosphere (CO_2 fertilization hypothesis) (LaMarche et al. 1984; Lewis et al. 2004; Cole et al. 2010). LaMarche et al. (1984) reported one of the first pieces of evidence of a possible CO_2 fertilization effect in tree rings of pines from the southwestern United States. Similarly, Lewis et al. (2004) hypothesized a cause-effect relationship between the increasing atmospheric CO_2 concentration and the observed increase in growth rates of the Amazon forest over the last few decades. A study on the growth of the aspen trees (*Populus* sp.) in a forest in Wisconsin (northern US) revealed an average increase of 53% over the past 5 decades in response to a 19.2% rise in ambient CO_2 levels (Cole et al. 2010).

Moore et al. (2006) observed a 13–27% increase in the basal area of *Pinus taeda* growing in Duke Forest, North Carolina (USA), exposed to elevated CO_2 for 8 yr. As evidenced by Bortoluzzi (2000), the degree of response of trees to elevated CO_2 may vary widely depending on species, growing conditions, nutrient availability, and the duration of the CO_2 enrichment, so it is not yet possible to generalize the available observations at a global level.

The effects of rising CO_2 concentration on tree growth rates have never been evaluated in the African continent. To contribute to filling this knowledge gap, the objective of the present study is to test the feasibility of a novel methodology based on ^{14}C measurements and tree-growth model fitting procedures for the estimation of biomass growth rate in trees from the most productive rain forest area in central Africa (in Cameroon). This approach should allow referring growth rates of wood to specific years without the help of ring counting analysis, thereby circumventing the problem of potential false or missing rings, which can be quite common in this geographical area.

MATERIALS AND METHODS

Study Site

The study site is Libongo (2°14′16″N and 16°9′59″E), in the eastern part of Lobeke National Park, Cameroon, which shares borders with the Central African Republic and the Republic of the Congo (Figure 1). The park is a semi-evergreen forest covering 2178.54 km^2, ranging from 300 to 750 m in altitude above mean sea level and hosting an enormous variety of plants including more than 300 tree species. The park has an annual rainfall averaging 1400 mm, with the dry season occurring from December through February, and an annual average temperature of 24 °C (Jell and Machado 2002). In 2010, individual trees of sapele, ayous, and tali were logged and some sections became available for further analyses. Radial subsections were sampled from these sections and used for ^{14}C analysis for growth rate determinations. The total length of each radial subsection from the pith to the cortex was measured to the nearest millimeter, and some samples (see below) were measured for ^{14}C abundances (see online Supplementary data).

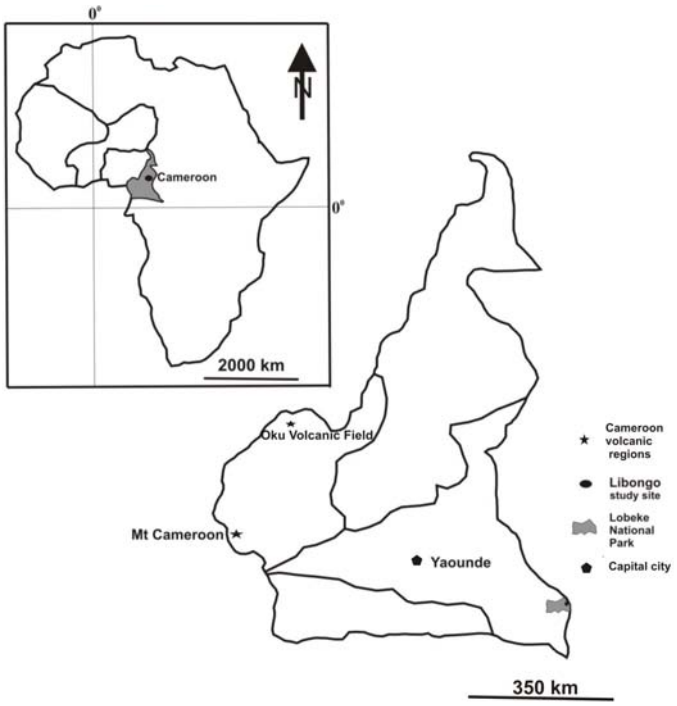

Figure 1 Map of Cameroon and location of the study site

Wood Sampling Approach

For each radial subsection, slices of about 2 mm in radial thickness were cut for ^{14}C measurements at different distances from the pith. Such sampled radial thickness represents a compromise between the minimum increment obtainable with our sampling instrumentation and the minimum mass of sample guaranteeing good statistics. Our main scope during the wood sampling was the reduction of possible long time periods (i.e. >1 yr) of pooling. Towards the outside of the radius, which was expected to be related to the bomb spike and enriched in modern ^{14}C, the sampling was denser.

Ayous and tali, respectively, were sampled sequentially from 15.4 to 38.1 cm and 31.9 to 43.8 cm from pith to cortex. Sapele was sequentially sampled from 9.3 to 44.7 cm (Sapele inner series) and 57.5 to 65.4 cm (Sapele outer series) from pith to cortex. Assuming that trees exhibit linear proportionality in growth in terms of height and radial increments and that density fluctuations over the tree life can be neglected, the cumulative biomass $M(r_i)$ in arbitrary units (a.u.) at a given distance from the pith (r_i) is proportional to

$$M(r_j) \propto 2\pi \sum_{i=1}^{j} r_i \cdot (r_i - r_{i-1}) = 2\pi \sum_{i=1}^{j} r_i \cdot \Delta r_i \quad (1)$$

where successive r_i represent mean sequential distances from the pith towards the cortex of the sample and Δr_i is the mean radial increment to which mass increments ($\Delta M(r_i)$) correspond in the time elapsed (Δt_i) between 2 considered samples. It is worth noting here that even if cumulative biomass is expressed in a.u. its increments exactly match the effective tree increments under the hypothesized conditions. In the modeling, we considered measured ^{14}C ages as a function of r_i with the aim to evaluate biomass growth rate ($\Delta M(r_i)/(\Delta t)$).

Sample Pretreatment and Radiocarbon Measurements

The α-cellulose was extracted from wood samples for all tree species using the modified Jayme-Wise method. α-cellulose was chosen because of its low mobility in wood, making annual ^{14}C signatures possible (Leavitt et al. 1993; Anchukaitis et al. 2008). During the applied procedure, acetic acid, initially used in addition with ($NaClO_2$) to remove lignin (Marzaioli et al. 2005), was replaced by HCl (Capano et al. 2010). The observed cellulose average mass yield of all samples was 39 ± 4.5% (average ± standard error) of the mass of bulk wood sample.

Three to 4 mg of extracted cellulose were oxidized to CO_2 via combustion in precleaned quartz tubes with copper oxide in muffle furnace at 920 °C for 6.5 hr. The CO_2 was then purified and graphitized, with Fe catalyst, using Zn and TiH_2 reagents in a muffle furnace at 560 °C for 8 hr (Marzaioli et al. 2008). Graphite was pressed into aluminum cathodes for ^{14}C analysis. ^{14}C measurements in this study were performed at the Center for Isotopic Research on the Cultural and Environmental Heritage (CIRCE) using a 3MV tandem accelerator (Terrasi et al. 2008). The $^{14}C/^{12}C$ isotopic ratio of each sample was corrected for 1) isotopic fractionation using on-line measured $^{13}C/^{12}C$, 2) background by means of Aesar zinc-processed fossil graphite, and 3) normalized to the ^{14}C activity of NIST OXII. Control standards (IAEA C3, C5, and C6; Rozanski et al. 1992) were measured to evaluate the entire procedure (preparation and measurement) accuracy. Measured ^{14}C abundances, for the purposes of this work, will be presented as $F^{14}C$ (Stuiver and Polach 1977) expressed in ‰ units.

Model for Growth Rates Estimation

Figure 2 illustrates the procedure for the estimation of the growth rates of sampled trees. First, ^{14}C measurements of sections of tree cores related to the distance from the pith, via Equation 1, were plotted as a function of the cumulative biomass $M(r_i)$ (panel I in Figure 2). $F^{14}C$ values versus biomass were attributed to calendar years by means of a sigmoid function (Equation 2) relating the wood biomass to calendar ages (panel II in Figure 2). This sigmoid function with 3 free parameters (α, β, γ) is assumed to reproduce the growth patterns of trees.

$$M(Yr;\alpha,\beta,\gamma) \propto \int_{-\infty}^{Yr} e^{\frac{-(Yr-\beta)^2}{2\gamma^2}} dYr \quad (2)$$

where α determines the maximum estimated biomass potentially fixed by the tree, β is the average age of the tree (i.e. the year of fixation of 50% of the asymptotic biomass), γ is proportional to the slope or growth rate of the tree, and *dYr* is the time differential.

For any value of the parameters α, β, and γ, the $(F^{14}C)_{meas}$ measured at distance from the pith r_i can be related to calendar ages by Equations 1 and 2 ($(F^{14}C)_{exp}$) and hence compared to the values in the calibration curve ($(F^{14}C)_{cal}$, panel III Figure 2). Then, the function

$$\chi^2 = \sum_{i=1}^{n} \frac{[(F^{14}C)_{exp} - (F^{14}C)_{cal}]}{s^2_{exp}}$$

(with s statistical uncertainty affecting $(F^{14}C)_{exp}$) can be minimized by varying α, β, and γ, yielding the M(Yr) curve that best fits the experimental data to the calibration curve. This procedure overcomes the problem of multiple solutions in the calibration curve arising from wiggles, the Suess effect, and the bomb spike.

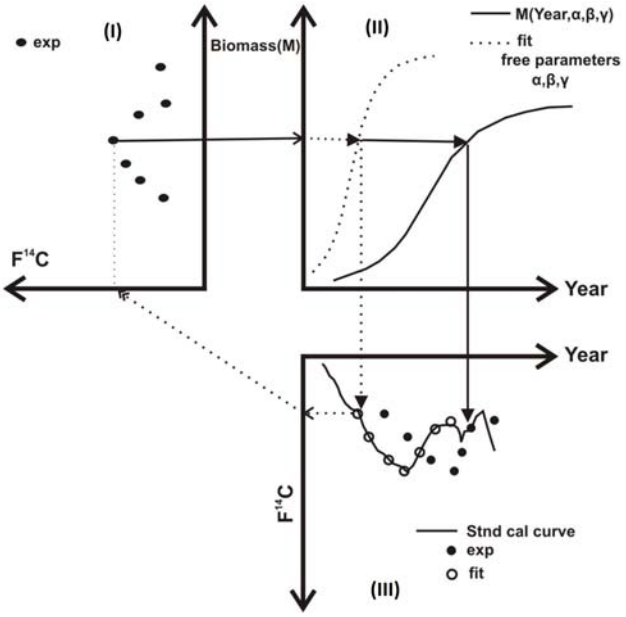

Figure 2 Schematic of the procedure applied for estimation of tree growth rates using ^{14}C measurements and tree growth models. Basically, a) each ^{14}C measurement is plotted versus the cumulative biomass by means of r_i and Equation 1 (panel I); b) cumulative biomass is related to absolute age by means of a sigmoid function (panel II); c) experimental $F^{14}C$ is compared with the standard calibration curve and differences minimized by changing sigmoid free parameters (α, β, and γ).

RESULTS AND DISCUSSIONS

Radiocarbon Analysis

Figure 3a shows the $F^{14}C$ values, in per mil modern carbon, measured for the subsamples from the trees as a function of the distance from the pith, r, in the part most affected by the bomb spike, i.e. close to the cortex. For comparison, Figure 3b shows the SH and NH3 records using the same vertical axis scale. In all 3 cases, the maximum experimental value in the bomb-peak region never exceeds 1650‰, contrary to the NH3 curve that exceeds 1650‰ between 1964 and 1967. Even if the horizontal scale in Figure 3a still has to be converted to calendar years (see below), it can be readily seen that our experimental data will be better fitted to the SH record than NH3. For this reason, we further considered the SH data set for comparison with our data, assuming that the same

holds also for the pre-bomb period, during which the difference between the 2 records is much smaller (McCormac et al. 2004). The same choice for bomb-spike data on Cameroon trees was done by Worbes et al. (2003), in spite of its geographical position, which according to Hua and Barbetti (2004), should be NH3.

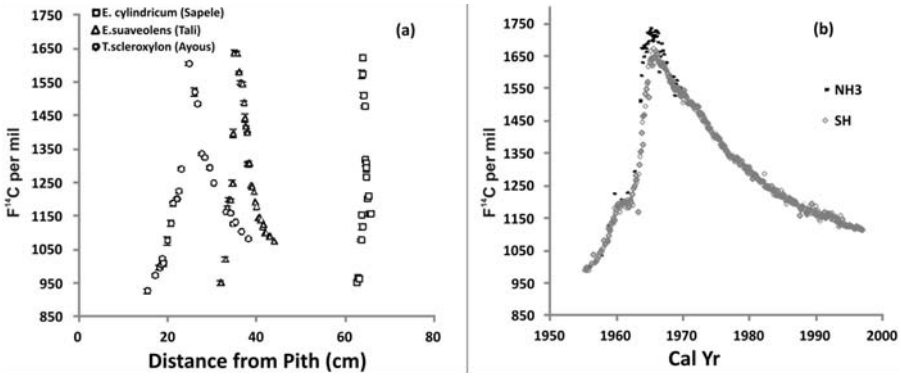

Figure 3 a) Radiocarbon $F^{14}C$ values of tree rings as a function of distance from pith in the bomb-spike years for sapele, tali, and ayous. b) $F^{14}C$ bomb-spike data sets for NH3 and SH (Hua and Barbetti 2004).

The ITCZ, at site latitudes, migrates north during the NH summer, generating a phase of low precipitations corresponding to the winter season (end of June to end of September) at the site. ITCZ southern migration instead generates also the SH summer stress (end of December to end of February), concentrating most of the photosynthetic activities in the periods corresponding to SH fall (end of March to end of June) and spring (end of September to end of December). Average ITCZ seasonal migration toward northern latitudes makes our site effectively fall under the SH in a period mostly at the end of April to end of October (Waliser 2002).

Given that the sampling of very narrow wood samples in radial sense was aimed mainly to avoid the pooling/averaging of long time periods (see above), the explanation for the agreement of ^{14}C ring data with the SH can be attributed to the fact that the most active period of CO_2 fixation by trees is concentrated during the period when the ITCZ migrates toward the NH. The observed data exclude possibilities of mixing between the CO_2 of the 2 hemispheres (NH, SH). This is evident by looking at the bomb-peak values recorded by each individual analyzed. In detail, one should note: 1) measured ^{14}C abundances never exceed the SH bomb-spike peak, as should be in case of sensitive mixing with the NH air; and 2) the NH/SH difference remains sensitive only for few years, compared to examined periods, after 1964 (Figure 3b).

Tree Growth Rates

As explained above, we adjusted the parameters of the biomass vs. year curve for the sapele tree in such a way that the $F^{14}C_{exp}$ vs. years data fit the SH data set $F^{14}C_{cal}$ vs. year, in the 13–47 cm and 57.6–65.4 ranges, using the SH pre-bomb (McCormac et al. 2004) and SH bomb spike (Hua and Barbetti 2004), respectively. In particular, the 2 biomass curves were constrained to match the same value at r = 57 cm. This is illustrated in Figure 4, where the experimental data are compared with those expected using the best-fit parameters $\alpha = 5350$, $\beta = 1846$, and $\gamma = 104$ in the first interval and $\alpha = 5070$, $\beta = 1805$, and $\gamma = 187$ in the second. The curve labeled *fit* represents the $F^{14}C$ values of the standard calibration curve obtained from the fit model corresponding to the distances of our measurements. Two anomalous ^{14}C points were observed (circled) in Figure 4. The possibility of these points being outliers was ruled out after a number of repeated measurements yielded the same

results within statistical uncertainties of the measurements. Cameroon is noted for several phases of volcanic activities, which are a source of depleted ^{14}C and can contribute to the presence of these ^{14}C-depleted points. Nevertheless, one cannot confirm with high certainty the probable relation between these points and the phases of volcanic activities in Cameroon; this is a result of the vast distance (>500 km) between our study site and the eruption sites (Figure 1), which is a critical factor that cannot be overlooked in this instance.

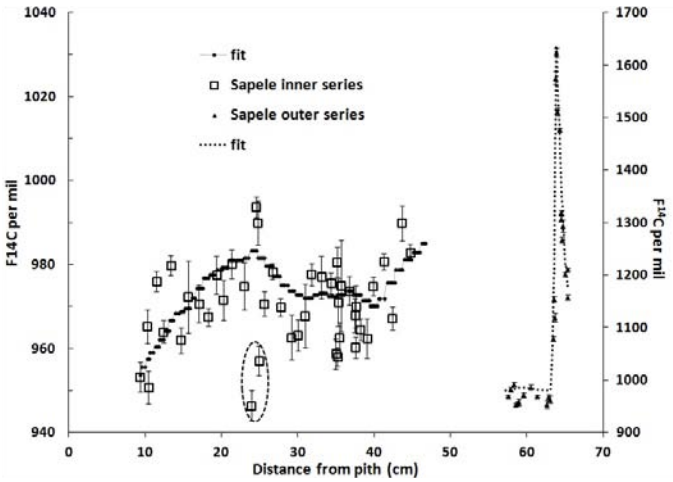

Figure 4 $F^{14}C$ pre- and post-bomb experimental data for the sapele cross-section compared with those expected using the best-fit model.

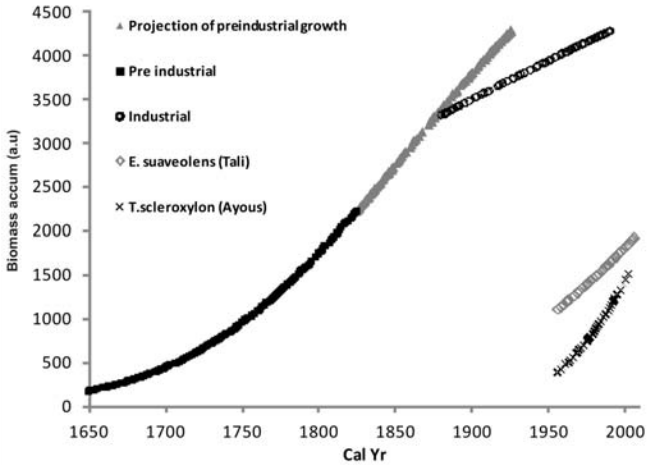

Figure 5 Best fits of growth patterns (in arbitrary units) of the sapele tree in the pre-industrial (squares) and industrial (circles) eras. Also shown are the extrapolation to the industrial era of the pre-industrial growth pattern (triangles) and industrial growth patterns for tali (diamonds) and ayous (crosses).

The best-fit biomass vs. cal yr curves are reported in Figure 5. For the sapele species, the slope of the fitted accumulated biomass curve, which represents the growth rate in the first and the second time intervals, is lower for the industrial period compared to the pre-industrial periods. This can be seen by comparing the extrapolation to the industrial period of the pre-industrial biomass sigmoid

curve with the post-industrial one fitting the bomb-spike period. It should be stressed here that one might expect slow growth in a young sapling, which tends to increase when it reaches canopy height, and slower growth in maturity. In our modeling, the pre-industrial curve and its projection take into account this effect, so experimental growth rates (referring to the industrial curve) seem to exacerbate the effect of slower growth rates within the tree maturity period. On the other hand, considering the CO_2 fertilization effects as argued by many reviews, a faster growth was to be expected in the industrial part of the curve. Nevertheless, no conclusion can be made from these data concerning possible CO_2 fertilization due to the fundamental absence of significant population sampling.

It must be noted that the results presented in this study do not include natural site variability being developed on single specimen analysis. For this reason, in order to draw a significant conclusion about the effect of CO_2 on the growth rate one should compare the growth rates estimated on more than 1 individual of the same species and the same age in the 2 different CO_2 environments (pre-industrial and industrial) to eliminate any aging effect that would retard the growth rate of trees at maturity. Indicated on the same plot are, for comparison, the growth patterns of the other 2 species, tali and ayous, estimated using the model. The mass increment per year in the 2 cases was, in the same arbitrary units employed for the sapele, 16 and 28 yr^{-1}, respectively, with sapele showing a value of 8 yr^{-1} for the post-industrial period. This difference could be attributed to a species-dependent growth rate as well as to an age effect, being the tali and ayous trees much younger than the sapele, even if a natural variability effect cannot be excluded. If, on the other hand, we consider the growth rate of the latter in the first phase of growth (7 yr^{-1}), this is in any case much lower than the other two. Nevertheless, no definite conclusion can be drawn about the eventual CO_2 fertilization effect, which would require analysis of a young sapele tree grown in the industrial era and a number of replicates.

CONCLUSIONS

Aiming to quantify the responses of the African rainforest to the ongoing climate change, trees from Cameroon were analyzed using a methodology that avoids any effects of the presence of false rings. Wood samples from 3 tree species from Cameroon were analyzed using ^{14}C measurements (AMS) at CIRCE from a total of 71 growth rings for *Entandrophragma cylindricum* (sapele), and 38 and 25 for *Erythrophleum suaveolens* (tali) and *T. scleroxylon* (ayous), respectively. A procedure was established and utilized for estimating the growth patterns of trees (purported not to have discernible annual rings) in the pre-industrial and industrial era. An old *Entandrophragma cylindricum* (sapele) specimen that dates from the pre-industrial to the industrial era was tested using this procedure. A decrease in the growth rates in the industrial era was observed compared to the pre-industrial era. Although this study has established that the procedure for estimating the effects of CO_2 on the growth patterns of trees in the pre-industrial and the industrial era in Cameroon is utilizable and feasible, the influence of atmospheric CO_2 levels on the growth patterns of the sapele tree species could not be conclusively determined. This is due to the possible effects introduced in the growth of trees by aging factor. Of course, this hypothesis should be verified on a significant sample of the populations of the tree. The authors believe that a comparison between pre- and post-industrial growth rates will require younger and older trees of the same species growing in the environment exposed to different CO_2 levels. This will eliminate any rate of growth introduced by the age of tree.

ACKNOWLEDGMENTS

This work was supported by European Research Council (ERC) grant 247349 Africa GHG. The authors are very grateful to Dr Simona Altieri for her enormous help during the sampling and preparation of wood samples, and to the referees whose suggestions helped improve the text.

REFERENCES

Anchukaitis KJ, Evans MN, Wheelwright NT, Schrag DP. 2008. Isotope chronology and climate signal calibration in neotropical cloud forest trees. *Journal of Geophysical Research* 113: G03030, doi:10.1029/2007JG000613.

Bortoluzzi B. 2000. Review of recent forest research projects on climate change and CO_2 concentration in Europe. European Forest Institute, Internal Report 1.

Cole CT, Anderson JE, Lindroth RL, Waller DM. 2010. Rising concentrations of atmospheric CO_2 have increased growth in natural stands of quaking aspen (*Populus tremuloides*). *Global Change Biology* 16(8): 2186–97.

Capano M, Marzaioli F, Sirignano C, Altieri S, Lubritto C, D'Onofrio C, Terrasi F. 2010. ^{14}C AMS measurements in tree rings to estimate local fossil CO_2 in Bosco Fontana forest (Mantova, Italy). *Nuclear Instruments and Methods in Physics Research B* 268(7–8):1113–6.

Currie K, Brailsford G, Nichol S, Gomez A, Riedel K, Sparks R, Lassey K. 2006. $^{14}CO_2$ in the Southern Hemisphere atmosphere – the rise and the fall. *Chemistry in New Zealand* 70(1):20–2.

Dunbar RB, Cole JE. 1999. Annual Records of Tropical Systems (ARTS), recommendations for research: Summary of scientific priorities and implementation strategies. Bern, Switzerland. PAGES workshop report 1999–1. 72 p.

Druffel ERM. 1997. Geochemistry of corals: proxies of past ocean chemistry, ocean circulation, and climate. *Proceedings of the National Academy of Sciences of the USA* 94(16):8354–61.

Fritts HC. 1976. *Tree Rings and Climate*. New York: Academic Press.

Hua Q, Barbetti M. 2004. Review of tropospheric bomb ^{14}C data for carbon cycle modeling and age calibration purposes. *Radiocarbon* 46(3):1273–98.

Hua Q, Barbetti M, Worbes M, Head J, Levchenko VA. 1999. Review of radiocarbon data from atmospheric and tree ring samples for the period 1950–1977. *IAWA Journal* 20(3):261–84.

Jell B, Machado JS. 2002. Collaborative management in the region of Lobeke, Cameroon: the potentials and constraints in involving the local population in protected area management. *Nomadic Peoples* 6:180–203.

LaMarche VC, Graybill DA, Fritts HC, Rose MR. 1984. Increasing atmospheric carbon dioxide: tree ring evidence for growth enhancement in natural vegetation. *Science* 225(4666):1019–21.

Lamoureux SF, Bradley RS. 1996. A 3300-year varved sediment record of environmental change from northern Ellesmere Island, Canada. *Journal of Paleolimnology* 16:239–55.

Leavitt SW. 1993. Seasonal $^{13}C/^{12}C$ changes in tree rings: species and site coherence, and a possible drought influence. *Canadian Journal of Forest Research* 23: 210–8.

Lewis SL, Phillips OL, Baker TR, Lloyd J, Malhi Y, Almeida S, et al. 2004. Concerted changes in tropical forest structure and dynamics: evidence from 50 South American long-term plots. *Philosophical Transactions of the Royal Society B* 359:421–6.

Marzaioli F, Lubritto C, Battipaglia G, Passariello I, Rubino M, Rogalla D. 2005. Reconstruction of past CO_2 concentration at a natural CO_2 vent site using radiocarbon dating of tree rings. *Radiocarbon* 47(2):257–63.

Marzaioli F, Borriello G, Passariello I, Lubritto C, De Cesare N, D'Onofrio A, Terrasi F. 2008. Zinc reduction as an alternative method for AMS radiocarbon dating: process optimization at CIRCE. *Radiocarbon* 50(1): 139–49.

McCormac FG, Hogg AG, Blackwell PG, Buck CE, Higham TFG, Reimer PJ. 2004. SHCal04 Southern Hemisphere calibration, 0–11.0 cal kyr BP. *Radiocarbon* 46(3):1087–92.

McCarroll D, Loader NJ. 2004. Stable isotopes in tree rings. *Quaternary Science Reviews* 23(7–8):771–801.

Moore DJP, Aref S, Ho RM, Pippen JS, Hamilton JG, De Lucia EH. 2006. Annual basal area increment and growth duration of Pinus taeda in response to eight years of free-air carbon dioxide enrichment. *Global Change Biology* 12(8):1367–77.

O'Brien SR, Mayewski PA, Meeker LD, Meese DA, Twickler MS, Whitlow SI. 1995. Complexity of Holocene climate as reconstructed from a Greenland ice core. *Science* 270(5244):1962–4.

Reimers NF. 1991. *The Popular Biological Dictionary.* Moscow: Nauka. 544 p. In Russian.

Rozanski K, Stichler W, Gonfiantini R, Scott EM, Beukens RP, Kromer B, van der Plicht J. 1992. The IAEA ^{14}C Intercomparison exercise 1990. *Radiocarbon* 34(3):506–19.

Stuiver M, Polach HA. 1977. Discussion: reporting of ^{14}C data. *Radiocarbon* 19(3):355–63.

Terrasi F, De Cesare N, D'Onofrio A, Lubritto C, Marzaioli F, Passariello I, Rogalla D, Sabbarese C, Borriello G, Casa C, Palmieri A. 2008. High precision ^{14}C AMS at CIRCE. *Nuclear Instruments and Methods in Physics Research B* 266(10):2221–4.

Waliser DE. 2002. Tropical meteorology: Intertropical convergence zones (ITCZ). In: Holdon J, Pyle J, Curry J, editors. *Encyclopedia of Atmospheric Sciences*. New York: Academic Press.

Whitmore TC. 1990. *An Introduction to Tropical Rain Forests.* Oxford: Clarendon Press.

Worbes M. 1989. Growth rings, increment and age of trees in inundation forests, savannas and a mountain forest in the Neotropics. *IAWA Bulletin* 10:109–22.

Worbes M, Staschel R, Roloff A, Junk WJ. 2003. Tree ring analysis reveals age structure, dynamics and wood production of a natural forest stand in Cameroon. *Forest Ecology Management* 173:105–23.